Published as: *DNA Repair (Amst)*. 2017 September ; 57: 133–138.

Synthetic lethality between murine DNA repair factors *XLF* and *DNA-PKcs* is rescued by inactivation of *Ku70*

Mengtan Xing[1], **Magnar Bjørås**[1], **Jeremy A. Daniel**[2], **Frederick W. Alt**[3,*], and **Valentyn Oksenych**[1,2,3,4,*]

[1]Institute for Cancer Research and Molecular Medicine, Norwegian University of Science and Technology, Laboratory Center, Erling Skjalgssons gate 1, 7491 Trondheim, Norway

[2]The NNF Center for Protein Research, Faculty of Health and Medical Sciences, University of Copenhagen, Blegdamsvej 3B, 2200 Copenhagen, Denmark

[3]Howard Hughes Medical Institute; Program in Cellular and Molecular Medicine, Boston Children'sHospital; Department of Genetics, Harvard Medical School, Boston, MA, 02115

[4]St. Olavs Hospital, Trondheim University Hospital, Clinic of Medicine, Postboks 3250 Sluppen, 7006 Trondheim

Abstract

DNA double-strand breaks (DSBs) are recognized and repaired by the Classical Non-Homologous End-Joining (C-NHEJ) and Homologous Recombination pathways. C-NHEJ includes the core Ku70 and Ku80 (or Ku86) heterodimer that binds DSBs and thus promotes recruitment of accessory downstream NHEJ factors XLF, PAXX, DNA-PKcs, Artemis and other core subunits, XRCC4 and DNA Ligase 4 (Lig4). In the absence of core C-NHEJ factors, DNA repair can be performed by Alternative End-Joining, which likely depends on DNA Ligase 1 and DNA Ligase 3. Genetic inactivation of C-NHEJ factors, such as *Ku70*, *Ku80*, *XLF*, *PAXX* and *DNA-PKcs* results in viable mice showing increased levels of genomic instability and sensitivity to DSBs. Knockouts of *XRCC4* or *Lig4*, on the other hand, as well as combined inactivation of *XLF* and *DNA-PKcs*, or *XLF* and *PAXX*, result in late embryonic lethality in mice, which in most cases correlate with severe apoptosis in the central nervous system. Here, we demonstrate that inactivation of the *Ku70* gene rescues the synthetic lethality between XLF and DNA-PKcs, resulting in triple knockout mice that are indistinguishable from Ku70-deficient littermates by size or levels of genomic instability. Moreover, we find that combined inactivation of *Ku70* and *XLF* results in viable mice. Together, these findings suggest that Ku70 is epistatic with XLF and DNA-PKcs and support a

[*]Corresponding: alt@enders.tch.harvard.edu (Frederick W. Alt). valentyn.oksenych@ntnu.no (Valentyn Oksenych).

Author contributions

MX, MB, JAD, FWA and VO designed and analyzed the experiments, the majority of which were performed by VO. MX and VO analyzed mouse genotypes and performed the T-FISH. VO wrote the manuscript. All the authors read and approved the final version of the manuscript.

model in which inactivation of Ku70 allows DNA lesions to become accessible to alternative DNA repair pathways.

Keywords

T-FISH; genomic instability; mouse genetics; epistasis; p53

1. Introduction

Non-Homologous DNA End Joining (NHEJ) is a cellular pathway that recognizes and fixes DNA double-strand breaks (DSBs) throughout the cell cycle. Core NHEJ factors include Ku70 and Ku80 (Ku86), a heterodimer that recognizes DSBs and has binding sites for multiple other NHEJ proteins. Ligation of DNA breaks is mediated by another heterodimer that includes core NHEJ factors, the DNA ligase 4 (Lig4) enzyme and its binding partner, XRCC4. DNA-dependent protein kinase, catalytic subunit (DNA-PKcs) and nuclease Artemis are accessory NHEJ factors, yet all of these proteins are individually required for lymphocyte development [1]. XRCC4-like factor (XLF) [2, 3] and paralog of XRCC4 and XLF (PAXX) [4–6] are NHEJ factors whose function remains to be determined.

Activation of the DNA damage response (DDR) signaling pathway occurs upon induction of DSBs. It consists of multiple enzymes responsible for posttranslational modifications as well as scaffold factors that are recruited to the chromatin areas adjacent to the DSBs. Related protein kinases *ataxia telangiectasia* mutated (ATM) and DNA-PKcs phosphorylate multiple substrates in response to DSBs, including histone H2AX and most of the NHEJ factors. Scaffold proteins MDC1 and 53BP1, ubiquitin ligases RNF8 and RNF168, and their downstream effectors RIF1 and PTIP then access modified chromatin [1].

Both NHEJ and the DDR are required for DNA repair events that are associated with the assembly of gene segments of immunoglobulins and T lymphocyte receptors, known as V(D)J recombination. During this process, Recombination Activating Gene (RAG) nuclease generates DSBs next to V, D and J gene segments, and NHEJ factors recognize and ligate DNA ends. Mature B lymphocytes change immunoglobulin isotypes in a process called Class Switch Recombination (CSR), when Activation induced Cytosine deaminase (AID) initiates DNA modifications that results in DSBs in the immunoglobulin constant region gene [1, 7]. CSR is also dependent on NHEJ and the DDR, although it can be robust, reaching about a half of wild type level, even in the absence of core NHEJ factors, likely due to the activity of DNA Ligase 1 and DNA ligase 3 [8, 9].

Mutations in several NHEJ factors in human are associated with developmental disorders that include immunodeficiency, neurological abnormalities and cancer [1]. A number of mouse knockouts were generated to model and investigate effects of NHEJ deficiency *in vivo*. *Ku70*- [10] and *Ku80*- [11] deficient mice are live-born, possess blocks in B and T lymphocyte development, and show moderate levels of p53-mediated apoptosis in central nervous system (CNS) [12]. Differently, deficiency for Lig4 or XRCC4 leads to p53-mediated late embryonic lethality in mice associated with high levels of apoptosis in the central nervous system [13–17]. Knockout of *DNA-PKcs* or *Artemis* results in live mice

with immunodeficiency due to defects in B and T lymphocyte development [18, 19], although a kinase dead (KD) mutation of DNA-PKcs results in embryonic lethality associated with neuronal apoptosis [20]. The *XLF* knockout results in nearly wild type mice with a mild reduction of lymphocyte count [21, 22], and knockout of PAXX does not lead to any detectable phenotype in mice [23, 24].

Inactivation of several NHEJ genes simultaneously allows studying genetic interactions within this pathway *in vivo*. For example, inactivation of *Ku80* rescued embryonic lethality of *Lig4*-deficient mice [25] and mice with catalytically dead DNA-PKcs [20]. Inactivation of *Ku70* also rescued lethality of *Lig4*-deficient mice [26, 27]; moreover, combined inactivation of *XLF* and *DNA-PKcs* [28] or *XLF* and *PAXX* resulted in synthetic lethality [23, 24].

XLF overlaps functionally with multiple factors in mouse development, lymphocyte development and maintenance of genomic stability. We and others have found that XLF-deficient lymphocytes are proficient in V(D)J recombination due to compensatory functions of other NHEJ factors, such as DNA-PKcs [28] and PAXX [23, 24, 29, 30]; the DDR factors, such as ATM and H2AX [31], 53BP1 [32, 33]; and RAG [34]. Combined inactivation of *XLF* and *H2AX* leads to early embryonic lethality [31], while mice with double deficiency of *DNA-PKcs* and *XLF* [28] or *PAXX* and *XLF* [23, 24] possess late embryonic lethality, resembling deficiency for *XRCC4* or *Lig4* [15, 16]. In the latter cases, the embryonic lethality is associated with massive cell death, including in the CNS. Besides functional overlap with XLF, DNA-PKcs is also functionally redundant with the related protein kinase ATM in aspects of mouse development, CSR and V(D)J recombination [35–37].

Here, we demonstrated that genetic inactivation of *Ku70* rescues embryonic lethality of *XLF*/*DNA-PKcs* double-deficient mice; moreover, combined inactivation of *Ku70* and *XLF* results in live mice phenotypically indistinguishable from *Ku70*-deficient littermates.

2. Materials and Methods

2.1. Mouse models

All experiments involving mice were performed according to the protocols approved by the Animal Resources Care Facility of Boston Children's Hospital (ARCH), University of Copenhagen and Norwegian University of Science and Technology (NTNU). $Ku70^{+/-}$ [10], $XLF^{+/\Delta}$ [21], DNA-$PKcs^{+/-}$ [16] and $p53^{+/-}$ [38] mice were previously described.

2.2. Tail fibroblasts

Primary murine tail fibroblasts were generated and cultured as described [28, 33]. Briefly, mouse tail skin was separated from the rest of the tail, cut into about 4 mm^2 pieces, and treated with 2 mg/mL collagenase II (Gibco) in DMEM supplemented with 15% (vol/vol) heat-inactivated FCS and antibiotics for 24 h at 37°C, at 5% (vol/vol) CO2 incubator. After being filtered through a 70-μm nylon cell strainer (BD Falcon), cells were washed in DMEM supplemented with 15% (vol/vol) FCS and plated. Fibroblasts from the second or third passages were used for telomere FISH assay.

2.3. Telomere FISH

Metaphases were prepared and chromosomal aberrations were counted as described [28, 33, 39]. The murine tail fibroblasts were synchronized with 100 ng/mL colcemid (KaryoMax, Gibco) for 6h. Then, the cells were treated with trypsin in PBS solution, washed with PBS, and lysed in 75 mM KCl (37°C, 20min). Fibroblasts were fixed in methanol:acetic acid (3:1) as described [39]. Telomeres were visualized with a Cy3-labeled fluorescent CCCTAACCCTAACCCTAA probe (Applied Biosystems). To visualize DNA, the samples were treated with DAPI (Vector Laboratories). Images were obtained with Eclipse microscope (Nikon). Chromosomal breaks were defined as a clear loss of telomere signal from both sister chromatids, and loss of telomere signal from one of the chromatids or clear absence of DAPI in the middle of one chromatid were defined as chromatid breaks.

3. Results

3.1. Generation of Ku70$^{-/-}$XLF$^{-/-}$ double deficient mice

Ku70 and Ku80 form a heterodimer (Ku) that recognizes DSBs and has affinity to other DNA repair factors, including the catalytic subunit DNA-PKcs forming the DNA-PK holoenzyme. In addition, Ku facilitates recruitment of XLF and PAXX to DSB sites [40, 41]. Mice with individual *Ku70*, *DNA-PKcs* or *XLF* genetic deficiencies are alive and possess different levels of genomic instability. Recently, we found that combined inactivation of *XLF* and *DNA-PKcs* leads to synthetic lethality, as XLF and DNA-PKcs have functional redundancy [1, 28] and (Fig. 1). To determine whether XLF functionally overlaps with either the entire DNA-PK complex or functions downstream and is dependent of Ku, we intercrossed mice homozygous for *XLF* null allele and heterozygous for *Ku70* (*Ku70*$^{+/-}$*XLF*$^{-/-}$). We obtained double knockout *Ku70*$^{-/-}$*XLF*$^{-/-}$ *Ku70*$^{-/-}$*XLF*$^{-/-}$ mice at the expected ratio, 25 out of 104 pups analyzed, or 24% (Fig. 1). In control cages, breeding of *DNA-PKcs*$^{+/-}$*XLF*$^{-/-}$ mice resulted in low number of live-born *DNA-PKcs*$^{-/-}$*XLF*$^{-/-}$ double knockout mice (5 out of 104 pups analyzed, or about 5%), and none of them lived longer than 5 days, P5 (Fig. 1). In addition, intercrossing of *Ku70*$^{+/-}$*DNA-PKcs*$^{+/-}$ mice resulted in alive *Ku70*$^{-/-}$*DNA-PKcs*$^{-/-}$ pups that were also born at a proportion close to expected (Fig. 1). We conclude that both XLF and DNA-PKcs function downstream of Ku70. Moreover, we did not observe any evidence of Ku70-independent function of XLF and DNA-PKcs *in vivo*.

3.2. Inactivation of Ku70 gene rescues perinatal lethality of XLF$^{-/-}$DNA-PKcs$^{-/-}$ mice

Upon interbreeding mice homozygous for *XLF* null allele and heterozygous for both *DNA-PKcs* and *Ku70* (*Ku70*$^{+/-}$*DNA-PKcs*$^{+/-}$*XLF*$^{-/-}$), triple null *Ku70*$^{-/-}$*DNA-PKcs*$^{-/-}$*XLF*$^{-/-}$ pups were surprisingly born at expected ratios, 17 out of 308, or about 5.5% (Fig. 2). These triple knockout mice were indistinguishable by size and lifespan from *Ku70*$^{-/-}$ or *Ku70*$^{-/-}$*XLF*$^{-/-}$ littermates (Fig. 3) and were alive up to 12 months of age. Meanwhile, there is a reduced number of live-born *XLF*$^{-/-}$*DNA-PKcs*$^{-/-}$ mice that rapidly died postnatally (by P5) when carrying one or two wild type alleles of *Ku70* (Fig. 2). In particular, there were about 2.6% of *Ku70*$^{+/+}$*DNA-PKcs*$^{-/-}$*XLF*$^{-/-}$ (8 out of 308) and 4.2% of *Ku70*$^{+/-}$*DNA-PKcs*$^{-/-}$*XLF*$^{-/-}$ (13 out of 308) pups born (Fig. 2). The average size of *Ku70*$^{-/-}$ mice at day P30 (8,2g) was similar to the ones of *Ku70*$^{-/-}$*XLF*$^{-/-}$ (8,5g), p=0.9987 and the size of triple

knockout *Ku70*$^{-/-}$*DNA-PKcs*$^{-/-}$*XLF*$^{-/-}$ mice (9,4g) was similar to double knockout *Ku70*$^{-/-}$*XLF*$^{-/-}$ (p=0.8328) and single knockout *Ku70*$^{-/-}$ (p=0.6506). See Figure legend for the full statistical comparisons between groups. We conclude that perinatal lethality of *XLF*$^{-/-}$*DNA-PKcs*$^{-/-}$ mice is Ku-dependent.

3.3. Ku70 is epistatic with XLF and DNA-PKcs in maintaining genomic stability

Combined deficiency for XLF and DNA-PKcs leads to high levels of genomic instability in murine fibroblasts measured as proportion of metaphases with chromosomal and chromatid breaks [28]. Should XLF have Ku-independent functions in maintaining genomic stability, we would expect an increased number of aberrant metaphases in *Ku70*$^{-/-}$*XLF*$^{-/-}$ cells compared to single *Ku70*$^{-/-}$ and *XLF*$^{-/-}$ cells. Here, we found that levels of genomic instability in *XLF*$^{-/-}$ and *DNA-PKcs*$^{-/-}$ primary murine tail fibroblasts are higher than in WT controls (Fig. 4). Moreover, the levels of genomic instability in *Ku70*$^{-/-}$ (25%), *Ku70*$^{-/-}$*XLF*$^{-/-}$ (28%) and *Ku70*$^{-/-}$*DNA-PKcs*$^{-/-}$*XLF*$^{-/-}$ (32%) fibroblasts are indistinguishable (p>0.2746), which suggests that *Ku70* is epistatic with both *XLF* and *DNA-PKcs* in maintaining genomic stability, and likely as a result of their functions in the NHEJ pathway. The levels of genomic instability in *DNA-PKcs*$^{-/-}$*XLF*$^{-/-}$ fibroblasts (26%) were similar to *Ku70*$^{-/-}$ cells, indicating that NHEJ is similarly abrogated in these two distinct genetic deficiencies (Fig. 4).

3.4. Haploinsufficiency for p53 rescues embryonic lethality of XLF$^{-/-}$DNA-PKcs$^{-/-}$ mice

By intercrossing mice homozygous for *XLF* null allele and heterozygous for both *DNA-PKcs* and *p53* (*DNA-PKcs*$^{+/-}$*XLF*$^{-/-}$*p53*$^{+/-}$), we found that inactivation of only one allele of *p53* results in live *DNA-PKcs*$^{-/-}$*XLF*$^{-/-}$*p53*$^{+/-}$ mice. Eight mice of this genotype were detected at 30 days postnatally in our studies. *DNA-PKcs*$^{-/-}$*XLF*$^{-/-}$*p53*$^{+/-}$ mice possessed reduced life span, which varied from 97 to 202 days, as well as reduced body weight being in the range of *Ku70*-deficient mice (data not shown). Further analyzis is required to determine how haploinsufficiency for *p53* rescues perinatal lethality of *DNA-PKcs*$^{-/-}$*XLF*$^{-/-}$ mice.

4. Discussion

4.1. Models to explain genetic interaction between Ku70, DNA-PKcs and XLF

The loss-of-function principle is widely used in current genetic studies of the NHEJ pathway. Traditionally, only one gene is inactivated; yet recent studies reveal that simultaneous inactivation of several genes is necessary to study functional overlap between proteins and to draw the most precise models of cellular pathways. Mice with inactivated *Ku70* and *Ku80* are alive but of smaller size than wild type littermates [10, 11]. Deficiency for *DNA-PKcs* or *XLF* leads to live-born mice with modest DNA repair defects [18, 21, 22]. DNA-PKcs forms the DNA-PK holoenzyme with the heterodimer Ku70/Ku80, and while the function of the catalytic subunit depends on the presence of Ku, inactivation of either the *Ku70* or *Ku80* gene will disrupt the whole DNA-PK complex [1, 42, 43]. Combined inactivation of *XLF* and *DNA-PKcs* leads to perinatal lethality in mice and abrogates NHEJ [28]. Here, we proposed and experimentally verified two models that would explain the genetic interaction between *Ku*, *DNA-PKcs* and *XLF* (Fig. 5). In one model, XLF has

functions in mouse development and DNA repair independent of Ku and potentially outside of NHEJ. In this case, XLF has functional redundancy with the entire DNA-PK holoenzyme, and combined inactivation of *Ku* and *XLF* would result in similar perinatal lethality as described for *DNA-PKcs*$^{-/-}$*XLF*$^{-/-}$ mice earlier [28]. In the other model, Ku recruits the downstream factors, including XLF and DNA-PKcs [1, 42, 43] and the function of XLF in mouse development and DNA repair completely depends on Ku. In this case, combined inactivation of *Ku70* and *XLF* genes would result in mice with a phenotype identical to those with single *Ku70* deficiency (Fig. 5, left panel). Indeed, our results strongly support the latter model. We found that the triple knockout *Ku70*$^{-/-}$*XLF*$^{-/-}$*DNA-PKcs*$^{-/-}$ mice are alive, and are nearly identical to *Ku70*$^{-/-}$ littermates by size and levels of genomic instability (Fig. 2–4). While the current manuscript was in the preparation, our colleagues found that combined inactivation of *Ku80* and *XLF* results in alive double knockout *Ku80*$^{-/-}$*XLF*$^{-/-}$ mice that resembles *Ku80*-knockout littermates [24].

4.2. Why does deficiency for Ku70 or p53 rescues perinatal lethality of DNA-PKcs$^{-/-}$XLF$^{-/-}$ mice?

Knockout of the upstream NHEJ genes *Ku70* or *Ku80* rescues embryonic lethality of mice with inactivated *Lig4* [25–27]. Here, we demonstrated a similar effect with inactivation of *Ku70* rescuing otherwise perinatally lethal *DNA-PKcs*$^{-/-}$*XLF*$^{-/-}$ double knockout mice. It is tempting to speculate that inactivation of *Ku70* or *Ku80* might also rescue the synthetic lethality between *XLF* and *PAXX* [23, 24], although this hypothesis remains to be tested. When one of the *Ku* genes is inactivated simultaneously with a downstream factor (*Lig4*, *XLF*, *DNA-PKcs*, etc.), the resulting phenotype reassembles *Ku70*$^{-/-}$ single knockout (Fig. 3, 4 and [25]). This suggests that the functions of downstream NHEJ factors is likely dependent on Ku. Indeed, there is no clear evidence of any Ku-independent function of these factors (XLF, PAXX, DNA-PKcs, Artemis, XRCC4 and Lig4) *in vivo*. With classical NHEJ is inactive in the absence of Ku70 or Ku80, the DSB sites become available for the alternative end-joining pathway(s). Although no significant difference exists between the genomic instability in *Ku70*$^{-/-}$ and *DNA-PKcs*$^{-/-}$*XLF*$^{-/-}$ fibroblasts (Fig. 4 and [28]), rescue of the lethal phenotype can be explained by a critical function of alternative end-joining in other organs, such as brain. For example, inactivation of *Lig4* or *XRCC4* can be more detrimental for the viability of neurons than inactivation of *Ku* [10, 13–16, 44].

Inactivation of one or two alleles of *Trp53* gene (*p53*) is also known to rescue the embryonic lethality associated with knockouts of downstream NHEJ factors XRCC4 and Lig4 [13, 14]. In this case, reduction of p53-dependent apoptosis may keep cells with accumulated DNA damages alive and extend the time necessary for alternative end joining to identify and fix a likely critical number of DSBs above a threshold that is compatible with life.

4.3. DNA-PKcs deficiency combined with XLF knockout

There are several mouse models with mutations in *DNA-PKcs* gene. The mice homozygous for catalytic dead DNA-PKcs (*DNA-PKcs*$^{KD/KD}$) possess embryonic lethality with high levels of genomic instability in affected embryos. This embryonic lethality is however rescued by combined inactivation of *Ku80* or *Ku70*, leading to alive *Ku80*$^{-/-}$*DNA-PKcs*$^{KD/KD}$ and *Ku70*$^{-/-}$*DNA-PKcs*$^{KD/KD}$ mice. Moreover, inactivation of one or two alleles

of *Trp53* gene also lead to alive $p53^{-/-}$*DNA-PKcs*$^{KD/KD}$ and $p53^{+/-}$*DNA-PKcs*$^{KD/KD}$ mice [20]. Complete knockout of *DNA-PKcs* [18] leads to live mice with no expressed DNA-PKcs protein; and a spontaneous mutation derived from the in inbred classical *SCID* mouse line also results in alive mice [45]. This latter mouse model carries minor modification at the C-terminus of the large DNA-PKcs subunit, which results in reduced amount of protein in the cells. In addition, this protein lacks its kinase activity. Thus, the SCID mouse model is distinct from the DNA-PKcs-null model, as it has residual amount of protein, albeit enzymatically inactive. Earlier, we have demonstrated that combined inactivation of *XLF* and *DNA-PKcs* results in perinatal lethality of *DNA-PKcs*$^{-/-}$*XLF*$^{-/-}$ mice. Moreover, chemical inhibition of DNA-PKcs kinase in *XLF*-deficient but not in WT pro-B cells completely blocks the joining of blunt signal ends (DSBs) at the chromosomal level [28]. There remains no mechanistic explanation of such a functional overlap between the DNA-PKcs and XLF. Whether or not inactivating *XLF* in the *SCID* mice would result in a similar synthetic lethality is an intriguing question. Such a double deficient model could be used in the future to explain whether functional overlap between XLF and DNA-PKcs is due to the structural or catalytic features of the DNA-PKcs.

Acknowledgments

This work was supported by National Institutes of Health (NIH) Grant AI076210 (to F.W.A.), and Research Council of Norway Young Talent Investigator grant # 249774 (to V.O.) F.W.A. is an investigator of the Howard Hughes Medical Institute. V.O. group is supported by The Liaison Committee for education, research and innovation in Central Norway (# 13477), the Cancer Society of Norway (# 182355), FRIMEDBIO grant (# 270491) and The Outstanding Academic Fellow Program (NTNU, 2017–2021). V.O. was a recipient of Lundbeck Foundation Research Fellowship (Denmark). Work in the laboratory of J.A.D. is supported by the Danish Council for Independent Research in Medical Sciences, the Danish Cancer Society, and grant to the Center for Protein Research from the Novo Nordisk Foundation (NNF14CC0001).

References

1. Kumar V, Alt FW, Oksenych V. Functional overlaps between XLF and the ATM-dependent DNA double strand break response. DNA Repair (Amst). 2014; 16:11–22. [PubMed: 24674624]
2. Buck D, et al. Cernunnos, a novel nonhomologous end-joining factor, is mutated in human immunodeficiency with microcephaly. Cell. 2006; 124(2):287–99. [PubMed: 16439204]
3. Ahnesorg P, Smith P, Jackson SP. XLF interacts with the XRCC4-DNA ligase IV complex to promote DNA nonhomologous end-joining. Cell. 2006; 124(2):301–13. [PubMed: 16439205]
4. Craxton A, et al. XLS (c9orf142) is a new component of mammalian DNA double-stranded break repair. Cell Death Differ. 2015; 22(6):890–7. [PubMed: 25941166]
5. Ochi T, et al. DNA repair. PAXX, a paralog of XRCC4 and XLF, interacts with Ku to promote DNA double-strand break repair. Science. 2015; 347(6218):185–8. [PubMed: 25574025]
6. Xing M, et al. Interactome analysis identifies a new paralogue of XRCC4 in non-homologous end joining DNA repair pathway. Nat Commun. 2015; 6:6233. [PubMed: 25670504]
7. Alt FW, et al. Mechanisms of programmed DNA lesions and genomic instability in the immune system. Cell. 2013; 152(3):417–29. [PubMed: 23374339]
8. Yan CT, et al. IgH class switching and translocations use a robust non-classical end-joining pathway. Nature. 2007; 449(7161):478–82. [PubMed: 17713479]
9. Boboila C, et al. Robust chromosomal DNA repair via alternative end-joining in the absence of X-ray repair cross-complementing protein 1 (XRCC1). Proc Natl Acad Sci U S A. 2012; 109(7):2473–8. [PubMed: 22308491]
10. Gu Y, et al. Growth retardation and leaky SCID phenotype of Ku70-deficient mice. Immunity. 1997; 7(5):653–65. [PubMed: 9390689]

11. Nussenzweig A, et al. Requirement for Ku80 in growth and immunoglobulin V(D)J recombination. Nature. 1996; 382(6591):551–5. [PubMed: 8700231]
12. Li H, et al. Deleting Ku70 is milder than deleting Ku80 in p53-mutant mice and cells. Oncogene. 2009; 28(16):1875–8. [PubMed: 19330025]
13. Gao Y, et al. Interplay of p53 and DNA-repair protein XRCC4 in tumorigenesis, genomic stability and development. Nature. 2000; 404(6780):897–900. [PubMed: 10786799]
14. Frank KM, et al. DNA ligase IV deficiency in mice leads to defective neurogenesis and embryonic lethality via the p53 pathway. Mol Cell. 2000; 5(6):993–1002. [PubMed: 10911993]
15. Frank KM, et al. Late embryonic lethality and impaired V(D)J recombination in mice lacking DNA ligase IV. Nature. 1998; 396(6707):173–7. [PubMed: 9823897]
16. Gao Y, et al. A critical role for DNA end-joining proteins in both lymphogenesis and neurogenesis. Cell. 1998; 95(7):891–902. [PubMed: 9875844]
17. Yan CT, et al. XRCC4 suppresses medulloblastomas with recurrent translocations in p53-deficient mice. Proc Natl Acad Sci U S A. 2006; 103(19):7378–83. [PubMed: 16670198]
18. Gao Y, et al. A targeted DNA-PKcs-null mutation reveals DNA-PK-independent functions for KU in V(D)J recombination. Immunity. 1998; 9(3):367–76. [PubMed: 9768756]
19. Rooney S, et al. Leaky Scid phenotype associated with defective V(D)J coding end processing in Artemis-deficient mice. Mol Cell. 2002; 10(6):1379–90. [PubMed: 12504013]
20. Jiang W, et al. Differential phosphorylation of DNA-PKcs regulates the interplay between end-processing and end-ligation during nonhomologous end-joining. Mol Cell. 2015; 58(1):172–85. [PubMed: 25818648]
21. Li G, et al. Lymphocyte-specific compensation for XLF/cernunnos end-joining functions in V(D)J recombination. Mol Cell. 2008; 31(5):631–40. [PubMed: 18775323]
22. Vera G, et al. Cernunnos deficiency reduces thymocyte life span and alters the T cell repertoire in mice and humans. Mol Cell Biol. 2013; 33(4):701–11. [PubMed: 23207905]
23. Liu X, et al. PAXX promotes KU accumulation at DNA breaks and is essential for end-joining in XLF-deficient mice. Nat Commun. 2017; 8:13816. [PubMed: 28051062]
24. Balmus G, et al. Synthetic lethality between PAXX and XLF in mammalian development. Genes Dev. 2016; 30(19):2152–2157. [PubMed: 27798842]
25. Karanjawala ZE, et al. The embryonic lethality in DNA ligase IV-deficient mice is rescued by deletion of Ku: implications for unifying the heterogeneous phenotypes of NHEJ mutants. DNA Repair (Amst). 2002; 1(12):1017–26. [PubMed: 12531011]
26. Boboila C, et al. Alternative end-joining catalyzes class switch recombination in the absence of both Ku70 and DNA ligase 4. J Exp Med. 2010; 207(2):417–27. [PubMed: 20142431]
27. Boboila C, et al. Alternative end-joining catalyzes robust IgH locus deletions and translocations in the combined absence of ligase 4 and Ku70. Proc Natl Acad Sci U S A. 2010; 107(7):3034–9. [PubMed: 20133803]
28. Oksenych V, et al. Functional redundancy between the XLF and DNA-PKcs DNA repair factors in V(D)J recombination and nonhomologous DNA end joining. Proc Natl Acad Sci U S A. 2013; 110(6):2234–9. [PubMed: 23345432]
29. Kumar V, Alt FW, Frock RL. PAXX and XLF DNA repair factors are functionally redundant in joining DNA breaks in a G1-arrested progenitor B-cell line. Proc Natl Acad Sci U S A. 2016; 113(38):10619–24. [PubMed: 27601633]
30. Lescale C, et al. Specific Roles of XRCC4 Paralogs PAXX and XLF during V(D)J Recombination. Cell Rep. 2016; 16(11):2967–79. [PubMed: 27601299]
31. Zha S, et al. ATM damage response and XLF repair factor are functionally redundant in joining DNA breaks. Nature. 2011; 469(7329):250–4. [PubMed: 21160472]
32. Liu XY, et al. Overlapping functions between XLF repair protein and 53BP1 DNA damage response factor in end joining and lymphocyte development. Proceedings of the National Academy of Sciences of the United States of America. 2012; 109(10):3903–3908. [PubMed: 22355127]
33. Oksenych V, et al. Functional redundancy between repair factor XLF and damage response mediator 53BP1 in V(D)J recombination and DNA repair. Proc Natl Acad Sci U S A. 2012; 109(7):2455–60. [PubMed: 22308489]

34. Lescale C, et al. RAG2 and XLF/Cernunnos interplay reveals a novel role for the RAG complex in DNA repair. Nat Commun. 2016; 7:10529. [PubMed: 26833222]
35. Callen E, et al. Essential Role for DNA-PKcs in DNA Double-Strand Break Repair and Apoptosis in ATM-Deficient Lymphocytes. Molecular Cell. 2009; 34(3):285–297. [PubMed: 19450527]
36. Zha S, et al. Ataxia telangiectasia-mutated protein and DNA-dependent protein kinase have complementary V(D)J recombination functions. Proc Natl Acad Sci U S A. 2011; 108(5):2028–33. [PubMed: 21245310]
37. Gapud EJ, et al. Ataxia telangiectasia mutated (Atm) and DNA-PKcs kinases have overlapping activities during chromosomal signal joint formation. Proc Natl Acad Sci U S A. 2011; 108(5): 2022–7. [PubMed: 21245316]
38. Jacks T, et al. Tumor Spectrum Analysis in P53-Mutant Mice. Current Biology. 1994; 4(1):1–7. [PubMed: 7922305]
39. Franco S, et al. H2AX prevents DNA breaks from progressing to chromosome breaks and translocations. Molecular Cell. 2006; 21(2):201–214. [PubMed: 16427010]
40. Tadi SK, et al. PAXX Is an Accessory c-NHEJ Factor that Associates with Ku70 and Has Overlapping Functions with XLF. Cell Rep. 2016; 17(2):541–555. [PubMed: 27705800]
41. Yano K, et al. Ku recruits XLF to DNA double-strand breaks. EMBO Rep. 2008; 9(1):91–6. [PubMed: 18064046]
42. Ochi T, Wu Q, Blundell TL. The spatial organization of non-homologous end joining: from bridging to end joining. DNA Repair (Amst). 2014; 17:98–109. [PubMed: 24636752]
43. Grundy GJ, et al. One ring to bring them all--the role of Ku in mammalian non-homologous end joining. DNA Repair (Amst). 2014; 17:30–8. [PubMed: 24680220]
44. Gu Y, et al. Defective embryonic neurogenesis in Ku-deficient but not DNA-dependent protein kinase catalytic subunit-deficient mice. Proc Natl Acad Sci U S A. 2000; 97(6):2668–73. [PubMed: 10716994]
45. Bosma GC, Custer RP, Bosma MJ. A severe combined immunodeficiency mutation in the mouse. Nature. 1983; 301(5900):527–30. [PubMed: 6823332]

Highlights

- Inactivation of *Ku70* gene rescues perinatal lethality of *XLF*$^{-/-}$*DNA-PKcs*$^{-/-}$ mice
- Inactivation of one allele of *Trp53* gene rescues perinatal lethality of *XLF*$^{-/-}$*DNA-PKcs*$^{-/-}$ mice
- *Ku70* is epistatic with *XLF* and *DNA-PKcs*
- Ku70$^{-/-}$, Ku70$^{-/-}$XLF$^{-/-}$ and Ku70$^{-/-}$DNA-PKcs$^{-/-}$XLF$^{-/-}$ mice are indistinguishable by size and levels of genomic instability.

Genotype	Number of offspring at day P30	Number of expected offspring (1:2:1)
DNA-PKcs$^{+/+}$XLF$^{-/-}$	36	26
DNA-PKcs$^{+/-}$XLF$^{-/-}$	63	52
DNA-PKcs$^{-/-}$XLF$^{-/-}$	0 (*5)	26
Ku70$^{+/+}$XLF$^{-/-}$	27	26
Ku70$^{+/-}$XLF$^{-/-}$	52	52
Ku70$^{-/-}$XLF$^{-/-}$	25	26
Ku70$^{+/+}$DNA-PKcs$^{-/-}$	13	10
Ku70$^{+/-}$DNA-PKcs$^{-/-}$	18	20
Ku70$^{-/-}$DNA-PKcs$^{-/-}$	8	10

*Live born pups that lived less than five days

Fig. 1. Double knockout *Ku70*$^{-/-}$*XLF*$^{-/-}$ mice are viable

The number of thirty-day-old mice (P30) of indicated genotypes. **Top.** Combined inactivation of *XLF* and *DNA-PKcs* leads to perinatal lethality. No DNA-PKcs$^{-/-}$XLF$^{-/-}$ mice survived longer than day P5 (*). **Middle.** Mice with combined inactivation of *Ku70* and *XLF* are live-born and develop as *Ku70*-deficient littermates. **Bottom.** Mice with combined inactivation of *Ku70* and *DNA-PKcs* are live-born and develop as *Ku70*-deficient littermates.

Genotype	Number of offspring at day P30	Number of expected offspring (1:2:1:2:4:2:1:2:1)
$Ku70^{+/+}$DNA-$PKcs^{+/+}XLF^{-/-}$	21	19
$Ku70^{+/+}$DNA-$PKcs^{+/-}XLF^{-/-}$	49	38
$Ku70^{+/+}$DNA-$PKcs^{-/-}XLF^{-/-}$	0 (*8)	19
$Ku70^{+/-}$DNA-$PKcs^{+/+}XLF^{-/-}$	50	38
$Ku70^{+/-}$DNA-$PKcs^{+/-}XLF^{-/-}$	91	76
$Ku70^{+/-}$DNA-$PKcs^{-/-}XLF^{-/-}$	0 (*13)	38
$Ku70^{-/-}$DNA-$PKcs^{+/+}XLF^{-/-}$	23	19
$Ku70^{-/-}$DNA-$PKcs^{+/-}XLF^{-/-}$	36	38
$Ku70^{-/-}$DNA-$PKcs^{-/-}XLF^{-/-}$	17	19

*Live born pups that lived less than five days

Fig. 2. Triple knockout *$Ku70^{-/-}$DNA-$PKcs^{-/-}XLF^{-/-}$* mice are viable

The number of thirty-day-old mice (P30) of indicated genotypes. Combined inactivation of *XLF* and *DNA-PKcs* leads to perinatal lethality of *$Ku70^{+/+}$* and *$Ku70^{+/-}$* mice with no mice survived longer than day P5 (*). Combined inactivation of *XLF, DNA-PKcs* and *Ku70* results in live-born mice that develop as *Ku70* single deficient littermates.

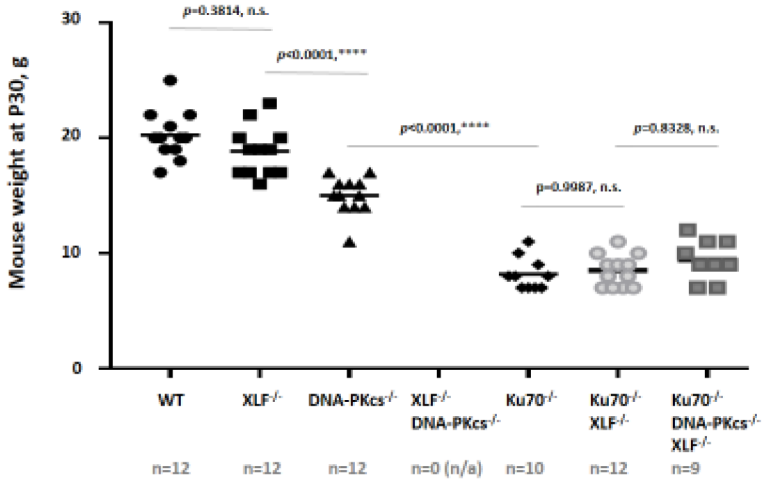

Fig. 3. Double knockout *Ku70*$^{-/-}$*XLF*$^{-/-}$ and triple knockout *Ku70*$^{-/-}$*DNA-PKcs*$^{-/-}$*XLF*$^{-/-}$ mice have similar size as *Ku70*$^{-/-}$ mice

Body weights of thirty-day-old mice (P30) of the indicated genotypes in grams.

The average weight of at least nine mice of each genotype is indicated. No *XLF*$^{-/-}$*DNA-PKcs*$^{-/-}$ were alive at day P30 (n=0; n/a=not available). The average size of wild type mice was 20,3g; 18,8g for *XLF*$^{-/-}$ mice and 15,0g for *DNA-PKcs*$^{-/-}$ mice. All *Ku70*-deficient mice were smaller. The average size of *Ku70*$^{-/-}$ mice (8,2g) was similar to the ones of *Ku70*$^{-/-}$*XLF*$^{-/-}$ (8,5g). The average size of triple knockout *Ku70*$^{-/-}$*DNA-PKcs*$^{-/-}$*XLF*$^{-/-}$ mice (9,4g) was similar to *Ku70*$^{-/-}$*XLF*$^{-/-}$ and *Ku70*$^{-/-}$.

Multiple comparisons between 15 groups with one-way ANOVA, GraphPad Prizm 7.03: **WT** *vs* XLF$^{-/-}$, p=0.3814 (n.s.); **WT** *vs* DNA-PKcs$^{-/-}$, p<0.0001 (****); **WT** *vs* Ku70$^{-/-}$, p<0.0001 (****); **WT** *vs* Ku70$^{-/-}$XLF$^{-/-}$, p<0.0001 (****); **WT** *vs* Ku70$^{-/-}$DNA-PKcs$^{-/-}$XLF$^{-/-}$, p<0.0001 (****); **XLF**$^{-/-}$ *vs* DNA-PKcs$^{-/-}$, p<0.0001 (****); **XLF**$^{-/-}$ *vs* Ku70$^{-/-}$, p<0.0001 (****); **XLF**$^{-/-}$ *vs* Ku70$^{-/-}$XLF$^{-/-}$, p<0.0001 (****); **XLF**$^{-/-}$ *vs* Ku70$^{-/-}$DNA-PKcs$^{-/-}$XLF$^{-/-}$, p<0.0001 (****); **DNA-PKcs**$^{-/-}$ *vs* Ku70$^{-/-}$, p<0.0001 (****); **DNA-PKcs**$^{-/-}$ *vs* Ku70$^{-/-}$XLF$^{-/-}$, p<0.0001 (****); **DNA-PKcs**$^{-/-}$ *vs* Ku70$^{-/-}$DNA-PKcs$^{-/-}$XLF$^{-/-}$, p<0.0001 (****); **Ku70**$^{-/-}$ *vs* Ku70$^{-/-}$XLF$^{-/-}$, p=0.9987 (n.s.); **Ku70**$^{-/-}$ *vs* Ku70$^{-/-}$DNA-PKcs$^{-/-}$XLF$^{-/-}$, p=0.6506 (n.s.); **Ku70**$^{-/-}$**XLF**$^{-/-}$ *vs* Ku70$^{-/-}$DNA-PKcs$^{-/-}$XLF$^{-/-}$, p=0.8328 (n.s.)

Genomic instability in tail fibroblasts

Genotype	Number of mice, n	Total metaphases,	Abnormal metaphases,		Chromosomal breaks,	Chromatid breaks,
		n	n	%	n	n
Wild type	5	250	14	2.8	9	1
XLF$^{-/-}$	5	250	30	12.0	24	8
DNA-PKcs$^{-/-}$	5	250	23	9.2	36	4
XLF$^{-/-}$DNA-PKcs$^{-/-}$	5	250	66	26.4	104	9
Ku70$^{-/-}$	3	150	38	25.3	49	12
XLF$^{-/-}$Ku70$^{-/-}$	5	250	69	27.6	93	17
XLF$^{-/-}$DNA-PKcs$^{-/-}$Ku70$^{-/-}$	4	200	65	32.5	97	15

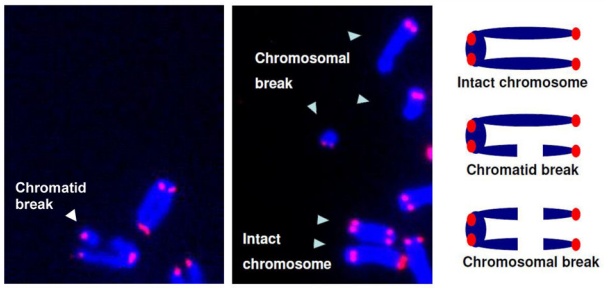

Fig. 4. Genomic instability in double knockout *Ku70*$^{-/-}$*XLF*$^{-/-}$ and triple knockout *Ku70*$^{-/-}$*DNA-PKcs*$^{-/-}$*XLF*$^{-/-}$ mice are similar to *Ku70*$^{-/-}$ mice

Analyses of genomic instability in primary tail fibroblasts.

Fibroblasts were isolated from live-born mice of indicated genotypes. **Top.** Number (n) and proportion (%) of metaphases with detected chromosomal or chromatid breaks in fibroblasts of indicated genotypes. Fifty metaphases per mouse and three to five mice per genotype were analyzed. **Bottom.** Examples of chromatid break, intact chromosomes and chromosomal breaks (left and middle). Schematic view of intact chromosome, chromatid break and chromosomal break (right).

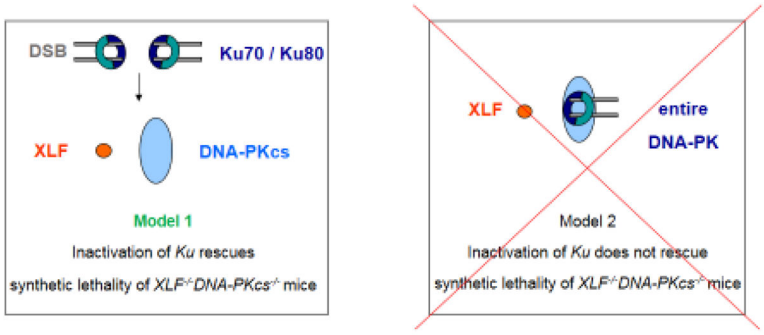

Fig. 5. Two models of functional interaction between the Ku, DNA-PKcs and XLF NHEJ factors

Left. Ku70/Ku80 heterodimer is recruited to the DNA break sites and facilitates recruitment of both XLF and DNA-PKcs. XLF has functional redundancy with DNA-PKcs, and inactivation of *Ku70* gene will rescue the perinatal lethality of $XLF^{-/-}DNA\text{-}PKcs^{-/-}$ double knockout mouse (this model is supported by our results). **Right.** Ku70/Ku80 is recruited to the DSB site and binds DNA-PKcs subunit to form a DNA-PK holoenzyme. Even though XLF recruitment to DSB is Ku-dependent, it could have Ku-independent function in mouse development, and thus functionally redundant with entire DNA-PK complex. Genetic inactivation of *Ku70* will not rescue the embryonic lethality of $XLF^{-/-}DNA\text{-}PKcs^{-/-}$ double-knockout mice (this model is not supported by our results).